ELSEVIER

www.elsevier.nl/locate/jorganchem

Journal of Organometallic Chemistry 607 (2000) 112–119

Journal of Organometallic Chemistry

2,6-Diphenylphenolates of calcium, strontium and barium exhibiting π-phenyl encapsulation of the partially naked cations

Glen B. Deacon [a,*], Craig M. Forsyth [a], Peter C. Junk [b]

[a] *Chemistry Department, Monash University, Clayton, Vic. 3168, Australia*
[b] *Department of Chemistry, James Cook University, Townsville, Qld. 4011, Australia*

Received 17 March 2000; received in revised form 29 April 2000

Dedicated to Professor Martin Bennett in recognition of his major contribution to organometallic chemistry and with thanks for his leadership in Australian chemistry.

Abstract

Solvent free 2,6-diphenylphenolates of calcium, strontium and barium have been prepared by direct reaction of the bulk metals with 2,6-diphenylphenol (HOdpp) at elevated temperatures in evacuated sealed tubes. Single-crystal X-ray diffraction studies of crystalline $[Ca_2(Odpp)_2(\mu\text{-}Odpp)_2]\cdot(PhMe)$ (**1**), $[Sr_2(Odpp)(\mu\text{-}Odpp)_3]\cdot(PhMe)$ (**2**) or $[Ba_2(Odpp)(\mu\text{-}Odpp)_3]$ (**3**), obtained by toluene extraction of the reaction mixtures, revealed different binuclear structural frameworks. In **1**, both Ca atoms have one terminal and two bridging aryloxide ligands in a pyramidal array with the coordination vacancies occupied by π-bonded pendant phenyl groups (an η^3- and an η^1-Ph on one Ca and an η^6-Ph on the other). By contrast, **2** has unsymmetrical metal–oxygen coordination with one terminal and three bridging aryloxides attached to one metal and solely three bridging aryloxides bound to the other. There are additional intramolecular π-Ph–Sr interactions with three η^1-Ph groups on the four coordinate Sr and three η^2-Ph groups on the three coordinate Sr. In **3**, the structure exhibits a similar metal–oxygen framework to **2**, but there are an increased number of π-phenyl–M interactions (one η^2-Ph and two η^1-Ph on the four coordinate Ba and one η^6-Ph, one η^3-Ph and one η^2-Ph on the three coordinate Ba).

Keywords: π-Phenyl complexes; Calcium; Strontium; Barium; Aryloxides

1. Introduction

π-Interactions of neutral arenes (or aryl moieties) with highly electropositive metal cations (e.g. Group 1 M^+, Group 2 M^{2+} and Group 3/lanthanide M^{3+} or M^{2+}) are rare but are becoming increasingly significant [1–3]. Although the bonding is weaker than for σ metal–phenyl interactions, and is characterised typically by long metal–carbon separations [1–3] (but within the sum of the van der Waals radii), they have the potential to influence the structural architecture of metal complexes. They also have implications for reactivity since their displacement may allow efficient entry of a weakly coordinating substrate into the metal coordination sphere. Observation of these features requires metals with vacant coordination sites, hence complexes of Groups 1–3 metals devoid of ancillary donors meet this criterion. Homoleptic phenoxides are appealing candidates, particularly where bulky substituents inhibit oligomerisation and reduce the number of bonded oxygen atoms to two (monomeric) or three (dimeric) for divalent ions. Whilst there have been some recent examples of bulky *ortho*-dialkylphenoxides of the larger Group 2 elements (Ca, Sr, Ba) [4–9], nearly all have additional coordinated solvents (giving metal coordination numbers ≥ 5). Examples without neutral donor ligands (or supporting donor substituents) are limited to $[M(OAr)_2]_2$ ($M = Ca$, Sr, Ba; $Ar = C_6H_2$-2,4,6-Bu^t_3) which were shown to be dimeric by molecular weight and ^{1}H-NMR measurements [6], consistent with the structurally characterised Mg derivative $[Mg(OAr)(\mu\text{-}OAr)]_2$ ($Ar = C_6H_2$-2,6-Bu^t_2-4-Me(H)) [10]. Following our successful syntheses of neutral-donor free lan-

* Corresponding author. Tel.: +61-3-99054568; fax: +61-3-99054597.
E-mail address: glen.deacon@sci.monash.edu.au (G.B. Deacon).

0022-328X/00/$ - see front matter
PII: S0022-328X(00)00262-X

thanoid 2,6-diphenylphenolates by direct reaction of the lanthanoid elements with 2,6-diphenylphenol (HOdpp) in the absence of a solvent, and the observation of intramolecular π-arene coordination to the lanthanoid centre [11,12], we now explore this approach to homoleptic aryloxides of the heavier Group 2 elements, Ca, Sr, and Ba as well as a preliminary examination of Mg.

2. Results and discussion

Elemental calcium, strontium, and barium, as well as magnesium react with HOdpp at 200–230°C in the presence of Hg to give colourless or pale yellow compounds which were isolated by extraction into toluene and crystallisation as the binuclear complexes $[M(Odpp)_2]_2$.(PhMe) (M = Ca (**1**), Sr (**2**)), $[Ba(Odpp)_2]_2$ (**3**) and the magnesium derivative $[Mg(Odpp)_2]$·(PhMe) (**4**) (Eq. (1)).

$$M(Hg) + 2HOdpp \rightarrow M(Odpp)_2 + H_2 \quad (1)$$

This procedure simplifies the conceptually related synthesis of X-ray uncharacterised $[M(OAr)_2]_2$ (M = Ca, Sr, Ba; Ar = C_6H_2-2,4,6-Bu^t_3) which utilised NH_3 to activate the metals [6]. Yields from reaction (1) were moderate to good (30–70%), the limitations being due to losses during crystallisation rather than incomplete reaction. Formation of aryloxo–metal complexes was evident by the absence of an OH stretching absorption in the infrared spectra of the products. An absorption band of 2,6-diphenylphenol at 827 cm^{-1}, which is shifted to 870–845 cm^{-1} in the $M(Odpp)_2$ complexes, cannot be attributed to γ(CH) of either phenyl groups or the three adjacent hydrogens of the phenolate ring [13], and is assigned to (predominantly) C–O deformation. The M = Mg, Ca complexes have two bands in the region (871, 850 (Mg); 862, 847 (Ca) cm^{-1}) whereas the M = Sr, Ba complexes have a single band at 849 cm^{-1}. The data appear indicative of two distinct structural types (see below). Mass spectra for M = Sr and Ba showed only $HOdpp^+$ (and fragment ions of HOdpp) but for M = Ca, ions due to the breakdown of a dimeric species were observed, consistent with the solid state structure established by X-ray crystallography (see below). The proton NMR spectrum of each complex showed, in addition to resonances of toluene where appropriate, a single Odpp environment indicative of a symmetrical monomeric species in solution (c.f. $[M(OAr)_2]_2$ (M = Ca, Sr, Ba; Ar = C_6H_2-2,4,6-Bu^t_3) which show resonances attributable to two distinct OAr groups in a 1:1 ratio [6]) or rapid exchange of the Odpp ligands. The complex $[Yb(Odpp)_2]_2$ [11], which is isostructural with $[Ca(Odpp)_2]_2$ and shows similar ^{1}H-NMR behaviour to the three $[M(Odpp)_2]_2$ complexes in C_6D_6, gave a low intensity, poorly resolved in the solvent region, uninterpretable ^{13}C-NMR spectrum for a solution in C_6D_6. Thus ^{13}C-NMR spectroscopy appears an ineffective probe for solution behaviour in non-polar media.

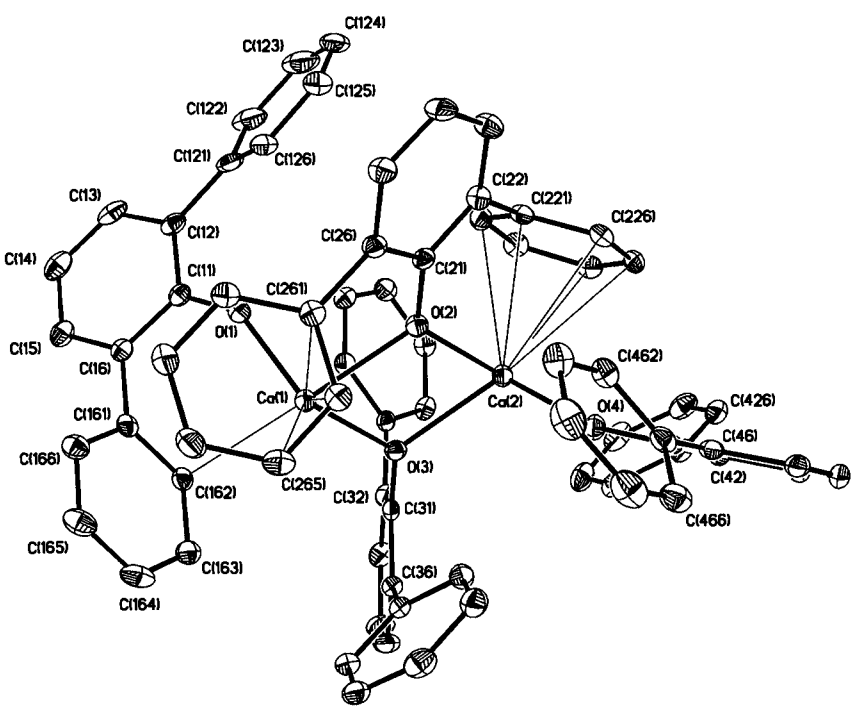

Fig. 1. The molecular structure of $[Ca_2(Odpp)_4]$·PhMe (**1**); hydrogens and the toluene of crystallisation have been omitted for clarity.

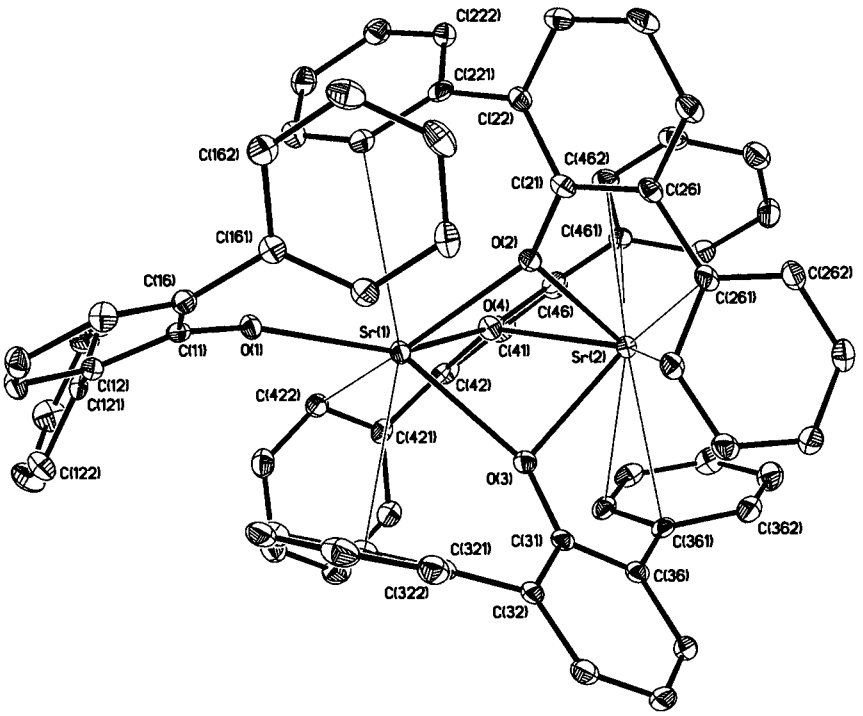

Fig. 2. The molecular structure of $[Sr_2(Odpp)_4]\cdot PhMe$ (**2**); hydrogens and the toluene of crystallisation have been omitted for clarity.

2.1. Single-crystal X-ray crystallography

The molecular structures of **1**–**3** (Figs. 1–4) were determined by single crystal X-ray diffraction methods. Crystal data are given in Table 1, selected bond distances and angles are listed in Tables 2–4. All three complexes were shown to be dinuclear, but two distinct metal–oxygen frameworks were observed. Thus, $[Ca_2(Odpp)_4]$ exhibits a classical dimeric structure with one terminal and two bridging aryloxide ligands at each metal (Fig. 1). In contrast, $[M_2(Odpp)_4]$ for M = Sr and Ba have one terminal and three bridging Odpp ligands at one metal centre and three bridging ligands at the other (Figs. 2 and 4) giving four and three coordinate metals, respectively. In all three structures, the metal–oxygen arrays leave much of the metals naked of primary donors and these vacancies are spectacularly filled by interactions with the phenyl substituents of the Odpp ligands.

The gross features of **1** and **2** are similar to those of the ytterbium(II) and europium(II) complexes $[Yb_2(Odpp)_4]$ and $[Eu(Odpp)(\mu\text{-}Odpp)_3]$ [11], respectively, as expected for metals of similar ionic radii and the same oxidation state [14]. Further, the Ca/Yb and Sr/Eu geometries (Tables 2 and 3 and Ref. [11]) are generally comparable although there are some minor variations between the $M–O_{br}$ distances and O–M–O angles in the Ca/Yb case. In terms of the M–O connectivity, the structures of **2** and **3** are also similar, despite the much larger radius of Ba^{2+} [14]. However, closer examination of the two structures reveals differences and these are discussed below.

The terminal Ca–O distances in **1** (Table 2) are somewhat shorter (0.07 Å) than those of $[Ca(OAr)_2(THF)_3]$ (Ar = C_6H_2-2,6-Bu^t_2-4-Me, THF = tetrahydrofuran) (2.181–2.210 Å) [4,5] but possibly less

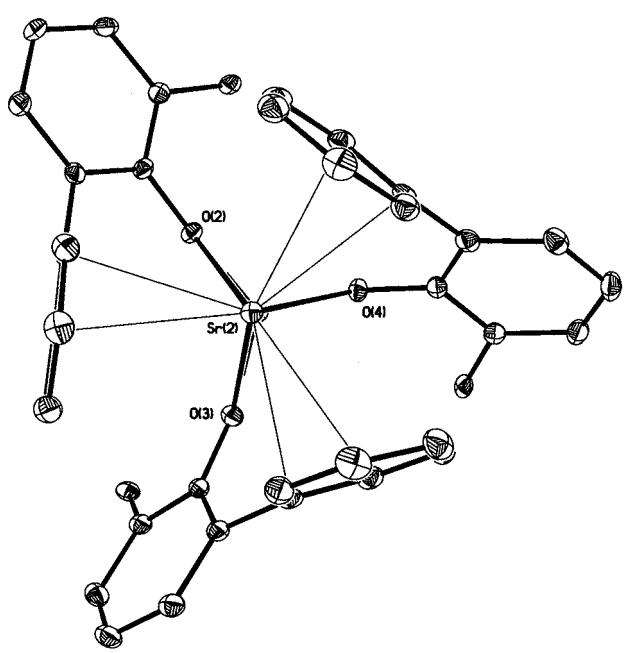

Fig. 3. View of **2** approximately down the Sr(2)···Sr(1) vector; the terminal Odpp and the 2-Ph of the remaining Odpp ligands have been omitted.

Table 1
Crystal and data collection parameters for **1**–**3**

	1·(PhMe)	**2**·(PhMe)	**3**
Formula	$C_{79}H_{60}Ca_2O_4$	$C_{79}H_{60}O_4Sr_2$	$C_{72}H_{52}Ba_2O_4$
Molecular weight	1153.43	1248.60	1255.87
Crystal system	Triclinic	Monoclinic	Orthorhombic
Space group	$P\bar{1}$	$P2_1/c$	*pbca*
a (Å)	12.0134(3)	18.0035(3)	19.4484(3)
b (Å)	12.8867(5)	15.1252(3)	15.2318(3)
c (Å)	19.7276(4)	21.4504(4)	37.1730(6)
α (°)	94.238(1)	90	90
β (°)	100.855(1)	90.997(1)	90
γ (°)	95.752(1)	90	90
V (Å^3)	2971(1)	5840(2)	11012(3)
Z	2	4	8
ρ_{calc} (g cm^{-3})	1.289	1.420	1.515
μ(Mo–K$_\alpha$) (mm^{-1})	0.246	1.882	1.474
Crystal size (mm)	$0.15\times0.18\times0.38$	$0.20\times0.25\times0.20$	$0.13\times0.20\times0.25$
$2\theta_{max}$ (°)	56.5	56.5	55.6
Unique reflections (R_{int})	13091 (0.041)	14417 (0.070)	10583 (0.044)
Reflections observed [$I>2\sigma(I)$]	7328	8892	6493
Data/restraints/parameters	13091/0/766	14471/0/766	10583/0/703
Goodness-of-fit (F^2)	1.008	1.027	1.022
R (*R* all data)	0.055 (0.128)	0.050 (0.112)	0.042 (0.103)
R_w (R_w all data)	0.117 (0.140)	0.078 (0.090)	0.067 (0.079)
Largest difference features (e Å^{-3})	0.43, −0.40	0.43, −0.50	0.88, −0.73

than anticipated on the basis of coordination numbers [14], suggestive of more than three coordination in **1** (see below). For **2** and **3**, the evidence for additional coordination is more marked, with the M–O$_{ter}$ distances (Tables 3 and 4) marginally *longer* than those of five coordinate [M(OAr)$_2$(THF)$_3$] (M = Sr, 2.323(10), 2.306(11) Å (Ar = C$_6$H$_2$-2,4,6-Bu$^t_3$) [6]; M = Ba, 2.38(1), 2.42(1) Å (Ar = C$_6$H$_2$-2,6-Bu$^t_2$-4-Me) [5]), despite the lower oxy-donor coordination numbers in **2** and **3**. As expected, the average M–O$_{br}$ distances are longer than M–O$_{ter}$ (Tables 2–4). Likewise, for **2** and **3**, <M–O$_{br}$> is shorter for the three coordinate metal than for the four coordinate metal. However, despite the situation for the average lengths, Sr(1)–O(2) and Sr(2)–O(2) are near equal and Ba(1)–O(2) is shorter than Ba(2)–O(2) despite Ba(2) having the lower coordination number (Tables 3 and 4). Moreover, in **2** and **3**, the sum of M(1)–O(*n*) and M(2)–O(*n*) is shorter for $n=2$ than $n=3$ or 4, notably more so for M = Ba, where O(2) has a significantly larger Ba(1)–O(*n*)–Ba(2) angle. A further feature of **3** is the marked asymmetry of the Ba–O–Ba bridges as exemplified by a 0.381 Å difference in the Ba(1)–O(4) and Ba(2)–O(4) distances. Comparison of the M–O$_{br}$ distances of **1**, **2**, and **3** with M-(μ_2-O) of the Group 2 metal phenoxide clusters, [Ca$_3$(OPh)$_5$(hmpa)$_6$]$^+$ (2.33(1)–2.36(1) Å [15]), [Sr$_4$(OPh)$_8$(THF)$_6$(PhOH)$_2$] (2.404(7)–2.495(7) Å [16]), [Sr$_3$(OPh)$_6$(hmpa)$_5$] (2.28(3)–2.53(2) Å [15]) and [Ba$_6$(OPh)$_{12}$(tmeda)$_4$] (2.619(3)–2.678(3) Å [15]) (hmpa = hexamethylphosphoramide, tmeda = *N*,*N*,*N*′,*N*′-tetramethylethane-1,2-diamine) shows that those of the clusters are longer for M = Ca, but are comparable or shorter for M = Sr and Ba despite the six-coordinate metals generally present in the clusters. These parallel trends in the M–O$_{ter}$ distances although some bond lengthening in **1**–**3** would be anticipated due to the higher steric requirements of Odpp relative to the unsubstituted phenoxy ligands.

In each of **1**, **2**, and **3**, there are considerable voids in the primary metal coordination spheres (Figs. 1, 2 and 4) and these are associated with a number of close contacts with some of the pendant phenyl groups of the Odpp ligands. In **1**, the coordination vacancies are identified clearly by the pyramidal CaO$_3$ arrays (c.f. triangular planar MgO$_3$ in [Mg(OAr)$_2$]$_2$, Ar = C$_6$H$_2$-2,6-Bu$^t_2$-4-Me(H) [10]). Even more remarkable are the three

Table 2
Selected bond distances (Å) and angles (°) in [Ca$_2$(Odpp)$_4$]·(PhMe) (**1**)

Bond distances			
Ca(1)–O(1)	2.122(2)	Ca(2)–O(4)	2.120(2)
Ca(1)–O(2)	2.275(2)	Ca(2)–O(2)	2.271(2)
Ca(1)–O(3)	2.249(2)	Ca(2)–O(3)	2.256(2)
Ca(1)···Ca(2)	3.582(1)		
Bond angles			
O(1)–Ca(1)–O(2)	96.62(6)	O(2)–Ca(2)–O(4)	103.30(7)
O(1)–Ca(1)–O(3)	112.24(7)	O(3)–Ca(2)–O(4)	113.18(6)
O(2)–Ca(1)–O(3)	75.32(6)	O(2)–Ca(2)–O(3)	75.25(6)
Ca(1)–O(2)–C(21)	126.1(1)	Ca(1)–O(3)–C(31)	130.4(1)
Ca(1)–O(2)–Ca(2)	103.98(7)	Ca(1)–O(3)–Ca(2)	105.31(7)
Ca(2)–O(2)–C(21)	129.3(1)	Ca(2)–O(3)–C(31)	124.3(1)

Table 3
Selected bond distances (Å) and angles (°) in $[Sr_2(Odpp)_4]\cdot(PhMe)$ (**2**)

Bond distances			
Sr(1)–O(1)	2.355(2)	Sr(1)···Sr(2)	3.5277(8)
Sr(1)–O(2)	2.432(2)	Sr(2)–O(2)	2.434(2)
Sr(1)–O(3)	2.498(2)	Sr(2)–O(3)	2.455(2)
Sr(1)–O(4)	2.499(2)	Sr(2)–O(4)	2.430(2)
Bond angles			
O(1)–Sr(1)–O(2)	123.31(6)	O(2)–Sr(2)–O(3)	78.29(6)
O(1)–Sr(1)–O(3)	143.19(6)	O(2)–Sr(2)–O(4)	72.65(6)
O(1)–Sr(1)–O(4)	140.70(6)	O(3)–Sr(2)–O(4)	73.15(6)
O(2)–Sr(1)–O(3)	77.50(6)	Sr(1)–O(2)–Sr(2)	92.95(6)
O(2)–Sr(1)–O(4)	71.48(6)	Sr(1)–O(3)–Sr(2)	90.85(6)
O(3)–Sr(1)–O(4)	71.25(6)	Sr(1)–O(4)–Sr(2)	91.39(6)
Sr(1)–O(2)–C(21)	147.1(2)	Sr(2)–O(2)–C(21)	119.9(2)
Sr(1)–O(3)–C(31)	150.4(2)	Sr(2)–O(3)–C(31)	116.2(2)
Sr(1)–O(4)–C(41)	148.5(2)	Sr(2)–O(4)–C(41)	118.2(2)

Table 4
Selected bond distances (Å) and angles (°) in $[Ba_2(Odpp)_4]$ (**3**)

Bond distances			
Ba(1)–O(1)	2.488(2)	Ba(1)···Ba(2)	3.9280(7)
Ba(1)–O(2)	2.559(2)	Ba(2)–O(2)	2.633(2)
Ba(1)–O(3)	2.804(2)	Ba(2)–O(3)	2.624(2)
Ba(1)–O(4)	2.887(2)	Ba(2)–O(4)	2.506(2)
Bond angles			
O(1)–Ba(1)–O(2)	96.98(8)	O(2)–Ba(2)–O(3)	76.99(7)
O(1)–Ba(1)–O(3)	140.19(7)	O(2)–Ba(2)–O(4)	70.84(7)
O(1)–Ba(1)–O(4)	146.25(7)	O(3)–Ba(2)–O(4)	74.54(7)
O(2)–Ba(1)–O(3)	75.05(7)	Ba(1)–O(2)–Ba(2)	98.31(8)
O(2)–Ba(1)–O(4)	66.01(7)	Ba(1)–O(3)–Ba(2)	92.65(7)
O(3)–Ba(1)–O(4)	66.19(7)	Ba(1)–O(4)–Ba(2)	93.24(7)
Ba(1)–O(2)–C(21)	145.6(2)	Ba(2)–O(2)–C(21)	114.0(2)
Ba(1)–O(3)–C(31)	131.0(2)	Ba(2)–O(3)–C(31)	134.2(2)
Ba(1)–O(4)–C(41)	127.7(2)	Ba(2)–O(4)–C(41)	138.4(2)

coordinate metals in **2** and **3**, which have only bridging Odpp ligands leaving a hemisphere on each metal unoccupied by oxygen donors. The metal–carbon distances that are considered to represent significant π-Ph–M interactions are listed in Table 5 along with the next nearest (non-bonding) distances for comparison. The bonding distance limits are derived from the complex reported recently $[(\eta^6\text{-PhMe})BaSn_3(\mu\text{-PSiBu}^t_3)_4]$ which has three Ba–P bonds and an η^6-PhMe–Ba fragment with Ba–C distances in the range 3.36–3.48 Å [17]. Subtraction of the differences in ionic radii between Ba^{2+} and Ca^{2+} or Sr^{2+} [14], give maximum metal–carbon distances of 3.13 or 3.30 Å for **1** and **2**, respectively. These are reasonable compared with the maximum Ln–C values for $[Yb_2(Odpp)_4]$ (3.18 Å) and $[Eu_2(Odpp)_4]$ (3.24 Å) [11], taking into account minor differences in ionic radii of the respective ions [14].

Thus, for **1**, there are an η^3-Ph and an η^1-Ph interaction with Ca(1) and an η^6-Ph with Ca(2). The next nearest Ca–C distance at 3.159 Å is only just outside the defined limit and may be considered as a further η^1-Ph interaction with Ca(2). The number of bonded carbon atoms is less than observed for $[Yb_2(Odpp)_4]$, (seven C at each Yb) [11] indicating a weaker coordination of the phenyl groups to calcium which may account for the wider O–Ca–O angles (thus deviating toward triangular) relative to the ytterbium structure [11].

The number of bonding carbon atoms at Sr(2) in **2** follows closely that of $[Eu_2(Odpp)_4]$ [11] with three η^2-Ph interactions. Interestingly, when viewed down the Sr···Sr vector (Fig. 3), it can be seen that these are staggered between the three Sr-(μ-O) bonds. At Sr(2), there are also close contacts with the *ipso* carbon atoms of the three bridging phenolate units (Table 5) but, although these distances are at or less than the defined maximum, they are longer than the Sr–C(phenyl) distances and may result from bending of the Odpp ligands toward Sr(2), which is evident from the larger Sr(1)–O(*n*)–C(*n*1) than Sr(2)–O(*n*)–C(*n*1) angles (Table 3), rather than a specific π-interaction with the phenolate ring. Three phenyl carbon atoms have distances to Sr(1) within the Sr–C bonding limits defining three η^1-Ph interactions, the same as observed for Eu(1) in $[Eu_2(Odpp)_4]$ [11]. The next nearest Sr–C(Ph) separation is 3.319 Å, approximately 0.2 Å longer than the two bonded carbon atoms of that particular phenyl ring.

The Ba complex **3**, possesses significantly more π-phenyl–metal interactions than observed for Sr in **2** with an η^6-Ph, an η^3-Ph and an η^2-Ph at Ba(2) (Fig. 4). The range of Ba–C values of the η^6-Ph–Ba fragment is wider than those of $[(\eta^6\text{-PhMe})BaSn_3(\mu\text{-PSiBu}^t_3)_4]$ [17], but they are generally shorter in **3**, indicating a stronger interaction. There are also two η^1-Ph and an η^2-Ph interacting with Ba(1), a slight increase in donor hapticity over Sr(1). In addition, C(425) is just outside the limit and may form part of a reasonable η^3-Ph–Ba(1) contact. The O(1)–Ba(1)···Ba(2) angle (137.79(6)°) is narrowed significantly toward O(2), more than the corresponding angle at Sr(1) in **2** (166.86(4)°), consistent with the greater number of π-phenyl interactions on Ba(1). As a consequence, the Odpp(2) ligand is tilted toward Ba(2) resulting in a close contact between C(21) and Ba(2). The other two bridging Odpp ligands are slightly tilted towards, rather than away from, the four coordinate Ba(1). The Ba(1)–O(*n*) ($n = 3$, 4) distances are significantly longer than Ba(1)–O(2) (Table 4), with the result that there is a lesser steric impact of the terminal Odpp on these ligands. There appears to be no correlation between the asymmetry of the bridging Ba–O distances and the degree of π-phenyl interaction since the Odpp ligand with the η^6-Ph has intermediate $Ba–O_{br}$ distances.

Because of the asymmetry of solid $[Ca_2(Odpp)_4]$, both in phase and out of phase, $Ca–O_{ter}$ deformation vibration of the two $Ca–O_{ter}$ bonds are infrared active, accounting for the two absorptions at 865–845 cm^{-1}. As $[Mg(Odpp)_2]$.PhMe has two similar bands, it may well have a similar structure. On the other hand, **2** and **3**, with only single $M–O_{ter}$ bonds, have only one absorption band in this range.

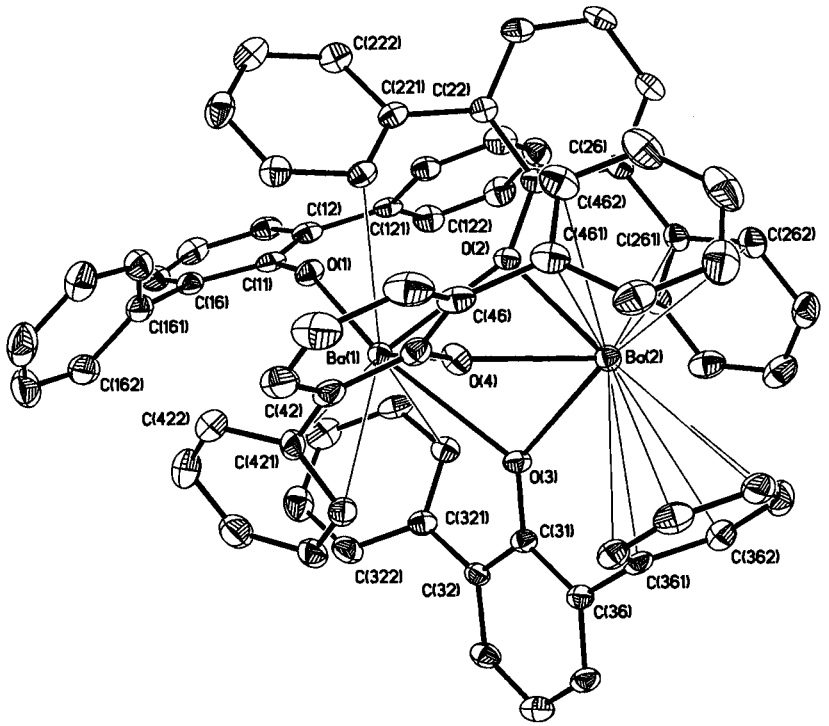

Fig. 4. The molecular structure of $[Ba_2(Odpp)_4]$ (**3**); hydrogens have been omitted for clarity.

Table 5
Metal–carbon distances (Å) of π-phenyl–metal interactions in **1**, **2**, and **3**

Bond distance					
Ca(1)–C(*n*)	(≤3.13 Å)	Sr(1)–C(*n*)	(≤3.30 Å)	Ba(1)–C(*n*)	(≤3.48 Å)
162	3.035(2)	226	3.225(3)	226	3.304(3)
261	2.946(3)	326	3.232(3)	326	3.225(3)
265	3.115(3)	422	3.100(3)	421	3.434(4)
266	2.790(3)			426	3.368(4)
Next nearest (non-bonded) distances					
Ca(1)···21	3.248(3)	Sr(1)···426	3.447(4)	Ba(1)···425	3.503(4)
Ca(2)–C(*n*)		Sr(2)–C(*n*)		Ba(2)–C(*n*)	
221	2.862(2)	261	2.986(3)	261	3.075(3)
222	2.843(3)	266	3.163(3)	262	3.251(4)
223	2.931(3)	361	3.026(3)	266	3.268(3)
224	3.034(2)	366	3.011(3)	361	3.204(3)
225	3.090(2)	461	3.050(3)	362	3.300(4)
226	3.000(2)	466	3.132(3)	363	3.407(4)
		21	3.302(3)	364	3.439(4)
		31	3.266(3)	365	3.356(4)
		41	3.268(3)	366	3.217(4)
				461	3.398(4)
				462	3.449(4)
				21	3.400(4)
Next nearest (non-bonded) distances					
Ca(2)···422	3.158(3)	Sr(2)···262	3.319(4)	Ba(2)···466	3.511(4)

3. Conclusions

The results described above show that the direct reaction of a mercury activated Group 2 metal with 2,6-diphenylphenol in the absence of a solvent provides an excellent route to homoleptic [M(Odpp)$_2$] complexes. We envisage that reactions of this type will have a wide application for the preparation of novel metal–organic complexes of Ca, Sr, and Ba (e.g. amides, phosphides and organometallics) and this is being pursued currently. Further, the success of these reactions demonstrates that novel metal-based synthetic methods developed for Group 3 and the lanthanoid elements can be readily transferred to the Group 2 metals. The homoleptic [M(Odpp)$_2$] complexes are sufficiently lacking in primary oxygen coordination that the metals exhibit rare (as yet!) examples of π-arene interactions with the pendant phenyl groups.

4. Experimental

The compounds described here are extremely air and moisture sensitive. All manipulations were carried out under purified (BASF R3/11 oxygen removal catalyst and activated 4 Å molecular sieves) nitrogen or argon using standard Schlenk techniques or in a vacuum atmospheres HE-43 dry box. Toluene was dried and deoxygenated by refluxing over blue sodium benzophenone ketyl under purified nitrogen. Elemental analyses (C, H) were performed by The Campbell Microanalytical Laboratory, Chemistry Department, University of Otago, Dunedin, New Zealand. IR spectra were obtained for Nujol mulls with a Perkin–Elmer 1600 FTIR instrument. For NMR spectra recorded on Bruker AC200 or AM300 spectrometers, data are reported relative to $SiMe_4$ and were referenced using the residual protonated solvent signals (C_6D_6 δ ^{1}H 7.15 ppm). Group 2 metals as turnings or pieces of distilled metal and 2,6-diphenylphenol were obtained from Aldrich and used as received.

4.1. Tetrakis(2,6-diphenylphenolato)dicalcium(II).(toluene) (1)

Calcium pieces (0.41 g, 10 mmol), mercury ($\sim$2 g) and HOdpp (1.04 g, 4.0 mmol) were placed in a thick walled Carius tube which was then evacuated to $< 10^{-3}$ mmHg and sealed. The reaction mixture was heated at 200°C for 48 h. The product was extracted with hot toluene (60 ml) and the colourless extract was reduced to 20 ml and allowed to stand at room temperature. Colourless crystals of the title compound deposited and were collected and dried under vacuum (yield 0.33 g, 29%). (Found: C, 82.3; H, 5.4. $C_{79}H_{60}Ca_2O_2$ requires C, 82.3; H, 5.6%). ν_{max} 1592m, 1558w, 1494m, 1415s, 1307m, 1278m, 1254m, 1176w, 1155w, 1070m, 1025w, 1010w, 862m, 847m, 800w, 765s, 748s, 736m, 711s, 700s 604m cm^{-1}. ^{1}H-NMR (C_6D_6): δ 2.10, s, 3H, CH_3 (toluene); 6.82, m, 28H, H4, H3′, H4′, H5′; 7.02, m, 5H, C_6H_5 (toluene); 7.19, d $^3J = 7.5$ Hz, 8H, H3, H5; 7.31, d $^3J = 6.5$ Hz, 16H, H2′, H6′.

4.2. Tetrakis(2,6-diphenylphenolato)distrontium(II)·(toluene) (2)

As above, strontium pieces (0.88 g, 10 mmol), mercury ($\sim$2 g) and HOdpp (1.04 g, 4.0 mmol) were heated to 200°C for 48 h. The product was extracted with hot toluene (60 ml). On cooling to room temperature, the extract deposited very pale yellow crystals of the title compound, which were collected and dried, under vacuum (yield 0.98 g, 78%). (Found: C, 76.2; H, 5.0. $C_{79}H_{60}O_2Sr_2$ requires C, 76.0; H, 4.8%). ν_{max} 1584m, 1556m, 1493m, 1408s, 1309w, 1284m, 1266m, 1231m, 1170w, 1157w, 1084m, 1068m, 1026w, 1010w, 849s, 804w, 758s, 746s, 734m, 710s, 598m cm^{-1}. ^{1}H-NMR (C_6D_6): δ 2.10, s, 3H, CH_3 (toluene); 6.74, t $^3J = 7.5$ Hz, 4H, H4; 6.84, br s, 24H, H3′, H4′, H5′; 7.02, m, 5H, C_6H_5 (toluene); 7.13 (overlapping residual protonated C_6D_6), H3, H5; 7.28, br s, 16H, H2′, H6′.

4.3. Tetrakis(2,6-diphenylphenolato)dibarium(II) (3)

As above, barium pieces (1.37 g, 10 mmol), mercury ($\sim$2 g) and HOdpp (1.04 g, 4.0 mmol) were heated to 200°C for 48 h. The product was extracted with hot toluene (60 ml). On cooling to room temperature, the extract deposited pale yellow crystals of the title compound, which were collected and dried, under vacuum (yield 0.51 g, 40%). (Found: C, 68.9; H, 4.1. $C_{72}H_{52}Ba_2O_2$ requires C, 68.9; H, 4.2%). ν_{max} 1584m, 1556m, 1493m, 1408s, 1309w, 1284m, 1266m, 1231m, 1170w, 1157w, 1084m, 1068m, 1026w, 1010w, 849s, 804w, 758s, 746s, 734m, 710s, 598m cm^{-1}. ^{1}H-NMR (C_6D_6): δ 6.73, t $^3J = 7.4$ Hz, 4H, H4; 6.85, m, 24H, H3′, H4′, H5′; 7.20, d $^3J = 7.6$ Hz, 8H, H3, H5; 7.37, br d $^3J \sim 7$ Hz, 16H, H2′, H6′.

4.4. Bis(2,6-diphenylphenolato)magnesium(II)·(toluene) (4)

As above, magnesium turnings (0.24 g, 10 mmol), mercury ($\sim$2 g) and HOdpp (1.04 g, 4.0 mmol) were heated at 200°C for 30 h. The product was extracted with toluene (40 ml) and the colourless extract was reduced to 10 ml and cooled to -20°C. Colourless crystals of the title compound deposited and were collected and dried under vacuum (yield 0.80 g, 66%). ν_{max} 1596m, 1565m, 1494m, 1420s, 1306m, 1298m, 1280w, 1238m, 1173w, 1157w, 1081w, 1069m, 1026w, 1010w, 994w, 932w, 871m, 850m, 804w, 758s, 751s, 731m,

715m, 702s, 634w, 604m, 591m cm^{-1}. ^{1}H-NMR (C_6D_6): δ 2.10, s, 3H, CH_3 (toluene); 6.88, m, 14H, H4, H3′, H4′, H5′; 7.02, m, 9H, C_6H_5 (toluene), H3, H5; 7.29, d $^3J = 6.3$ Hz, 8H, H2′, H6′.

4.5. Structure determinations

Representative single crystals were covered in heavy oil and mounted on an Enraf–Nonius CCD diffractometer and cooled in a nitrogen stream. Hemispheres of data were collected using ϕ scans or a combination of ϕ and ω scans at 1° per frame. The raw diffraction images were integrated and scaled using the Nonius proprietary software package (DENZO-SMN) [18] yielding N independent reflections which were used in the full-matrix least-squares refinement (SHELX 97) [19]. Anisotropic thermal parameter forms were refined for the non-hydrogen atoms and hydrogen atoms were included in calculated positions with thermal parameters allowed to ride on the parent carbon.

Acknowledgements

We are grateful to the Australian Research Council for financial support.

References

[1] C. Schade, P. von R. Schleyer, Adv. Organomet. Chem. 27 (1987) 169.
[2] W.E. Lindsell, in: E.W. Abel, F.G.A. Stone, G. Wilkinson (Eds.), Comprehensive Organometallic Chemistry II, vol. 1, Pergamon, Oxford, 1995, p. 57 Chap. 3.
[3] G.B. Deacon, Q. Shen, J. Organomet. Chem. 511 (1996) 1.
[4] P.B. Hitchcock, M.F. Lappert, G.A. Lawless, B. Royo, J. Chem. Soc. Chem. Commun. (1990) 1141.
[5] K.F. Tesh, T.P. Hanusa, J.C. Huffman, C.J. Huffman, Inorg. Chem. 31 (1992) 5572.
[6] S.R. Drake, D.J. Otway, M.B. Hursthouse, K.M. Abdul Malik, Polyhedron 11 (1992) 1995.
[7] P. Miele, J.-D. Foulon, N. Hovnanian, L. Cot, Polyhedron 12 (1993) 267.
[8] T.R. Bellderrain, J.P. Espinoa, A. Fernandez, A.R. Gonzalez-Elipe, D. Leinen, A. Monge, M. Paneque, C. Ruiz, E. Caroma, J. Chem. Soc. Dalton Trans. (1995) 1529.
[9] W.J. Evans, W.G. McClelland, M.A. Greci, J.W. Ziller, Eur. J. Solid State Inorg. Chem. 33 (1996) 1970.
[10] J.C. Calabrese, M.A. Cushing Jr., S.D. Ittel, Inorg. Chem. 27 (1988) 867.
[11] G.B. Deacon, C.M. Forsyth, P.C. Junk, B.W. Skelton, A.H. White, Chem. Eur. J. 5 (1999) 1452.
[12] G.B. Deacon, C.M. Forsyth, A. Gitlits, B.W. Skelton, A.H. White, J. Chem. Soc. Dalton Trans. (2000) 961.
[13] L.J. Bellamy, The Infrared Spectra of Complex Molecules, second ed., Wiley, New York, 1964, p. 78.
[14] R.D. Shannon, Acta Crystallogr. Sect. A 32 (1976) 751.
[15] K.G. Caulton, M.H. Chisholm, S.R. Drake, K. Folting, J.C. Huffman, W.E. Streib, Inorg. Chem. 32 (1993) 1970.
[16] S.R. Drake, W.E. Streib, M.H. Chisholm, K.G. Caulton, Inorg. Chem. 29 (1990) 2707.
[17] M. Westerhausen, M. Krofta, N. Wiberg, J. Knizck, H. North, A. Pfitzner, Z. Naturforsch. B53 (1998) 1489.
[18] Z. Otwinowski, W. Minor, in: C.W. Carter Jr., R.M. Sweet (Eds.), Methods in Enzymology. Part A, vol. 276, Academic, New York, 1997, p. 307.
[19] G.M. Sheldrick, SHELX97, Program for Crystal Structure Determination, University of Göttingen, Germany, 1997.